

Effect of Europium Ion on Pseudoboehmite Phase Transition and Microstructure

Zhu Fuliang¹, Meng Yanshuang¹, Wang Dajian²

¹ State Key Laboratory of Gansu Advanced Non-ferrous Metal Materials, Lanzhou University of Technology, Lanzhou 730050, China; ² Tianjin University of Technology, Tianjin 300384, China

Abstract: After doping $\text{Eu}(\text{NO}_3)_3$ into pseudoboehmite sol suspension, europium-doped pseudoboehmite xerogel was prepared by a spray-drying process. Effects of Eu^{3+} ions on pseudoboehmite phase transition and microstructure were investigated by differential thermal gravimetric analysis, X-ray powder diffraction and field emission transmission electron microscopy. Results show that upon doping of Eu^{3+} ions into pseudoboehmite, the phase transition temperatures of $\gamma\text{-Al}_2\text{O}_3 \rightarrow \theta\text{-Al}_2\text{O}_3$ and $\theta\text{-Al}_2\text{O}_3 \rightarrow \alpha\text{-Al}_2\text{O}_3$ increase by 172 °C and 13 °C, respectively. It is found that Eu^{3+} ions entirely enter $\gamma\text{-Al}_2\text{O}_3$ or $\theta\text{-Al}_2\text{O}_3$ crystal lattices, and the crystallinity of $\gamma\text{-Al}_2\text{O}_3$ is improved, resulting in increasing of the phase transition temperature of $\gamma\text{-Al}_2\text{O}_3 \rightarrow \theta\text{-Al}_2\text{O}_3$. When $\alpha\text{-Al}_2\text{O}_3$ is generated in the phase transition process, all of Eu^{3+} ions exist among $\alpha\text{-Al}_2\text{O}_3$ grain boundaries in the form of compound $\text{EuAl}_{12}\text{O}_{19}$, which will hinder the bulk diffusion of Al^{3+} resulting in an increase of phase transformation temperature of $\theta\text{-Al}_2\text{O}_3 \rightarrow \alpha\text{-Al}_2\text{O}_3$ process.

Key words: pseudoboehmite; phase transition; Eu^{3+} doped; microstructure

Pseudoboehmite (AlOOH) is a crystal imperfect boehmite. When pseudoboehmite is calcined at 400–700 °C, product $\gamma\text{-Al}_2\text{O}_3$ is widely used as a catalyst carrier, catalyst and adsorbent. Nano $\alpha\text{-Al}_2\text{O}_3$, obtained by sintering pseudoboehmite at 1200 °C, is extensively employed as a paint additive, top-grade ceramic, petrochemical efficient catalyst, sub-micron/nano abrasive and polishing materials, cosmetic filling materials and inorganic membrane materials. The study of pseudoboehmite phase transition on its application has received extensive attentions^[1,2].

Phase transition temperatures of $\gamma\text{-Al}_2\text{O}_3 \rightarrow \theta\text{-Al}_2\text{O}_3$ and $\theta\text{-Al}_2\text{O}_3 \rightarrow \alpha\text{-Al}_2\text{O}_3$ can be changed by adding metal ionic salts or metal oxides, which are reported in the literatures^[3–25]. According to the literature survey, additions of B_2O_3 , La_2O_3 , Y_2O_3 , CaO and salts of Ba , Sr and Ca can elevate phase transition temperature of $\theta\text{-Al}_2\text{O}_3 \rightarrow \alpha\text{-Al}_2\text{O}_3$. Additions of Fe_2O_3 , $\text{CuO/Cu}_2\text{O}$, TiO_2 , V_2O_5 , MgAl_2O_4 , $\gamma\text{-Al}_2\text{O}_3$ and $\alpha\text{-Al}_2\text{O}_3$ can reduce phase transition temperature of $\theta\text{-Al}_2\text{O}_3 \rightarrow \alpha\text{-Al}_2\text{O}_3$. Additions of Ta_2O_5 , Li_2O and MgO have

no apparent effect on phase transition temperature of $\theta\text{-Al}_2\text{O}_3 \rightarrow \alpha\text{-Al}_2\text{O}_3$. Effects of Cr_2O_3 , SiO_2 and ZrO_2 on phase transition temperature of $\theta\text{-Al}_2\text{O}_3 \rightarrow \alpha\text{-Al}_2\text{O}_3$ are under way to be further studied.

Effects of Eu^{3+} ions on phase transition temperature of pseudoboehmite have not been reported yet in literature. Therefore, we would like to conduct the above mentioned investigation so as to provide technical evidence for pseudoboehmite applications in various fields.

1 Experiment

Pseudoboehmite powder supplied by the Aluminum Corporation of China Limited was prepared by a HNO_3 peptization method. The reagents were HNO_3 (analytical purity reagent) and $\text{Eu}(\text{NO}_3)_3$ (analytical purity reagent). AlOOH powder and redistilled water were mixed according to their stoichiometry and agitated to produce a suspension of solid content of 5% AlOOH . The suspension was continuously stirred and 5 mol/L nitric acid solution was

Received date: August 27, 2014

Foundation item: National Natural Science Foundation of China (51364024, 50364002); Foundation of State Key Laboratory of Gansu Advanced Non-ferrous Metal Materials (SKL 1316); Gansu Province Department of Education Fund (2013A-029)

Corresponding author: Meng Yanshuang, Ph. D., Associate Professor, State Key Laboratory of Gansu Advanced Non-ferrous Metal Materials, Lanzhou University of Technology, Lanzhou 730050, P. R. China, Tel: 0086-931-2936378

Copyright © 2015, Northwest Institute for Nonferrous Metal Research. Published by Elsevier BV. All rights reserved.

added simultaneously to produce AIOOH colloid under the conditions of pH = 2 and stirring time for 3 h. AIOOH gel was obtained through drying and spraying by SD-06 spray dryer (Labplant, UK). And the sample obtained was labeled as Sp. $\text{Eu}(\text{NO}_3)_3$ with a molar ratio of $\text{Eu}(\text{NO}_3)_3:\text{AIOOH} = 0.02:1$ was proposed to AIOOH colloidal suspension. $\text{Eu}(\text{NO}_3)_3$ was fully dispersed into AIOOH sol via stirring for 1 h. Eu^{3+} doped AIOOH sample (labeled as Sp-E) was dried and sprayed by the spray dryer as mentioned above. Spray drying conditions were determined as follows: the colloidal suspension flow of 15 mL/min, air temperature of 150 °C and the sample outlet temperature of 62 °C. Samples of Sp and Sp-E were sintered at 600, 900 °C, 1100 and 1300 °C, under ambient condition for 3 h with heating rate of 10 °C/min GSL1600X tube furnace.

XRD analysis of the samples was conducted by a D/max-2500/PC type XRD diffractometry (Rigaku, Japan). Differential thermal gravimetric analysis (TG/DSC) of the sample was carried out using a STA 449C type thermal analyser (Netsch, Germany). The sample (about 15 mg) was placed into the platinum crucible under N_2 atmosphere with a flow rate of 15 mL/min, heating rate of 10 °C/min and the detection temperature range of 40 °C to 1500 °C. Morphologies of samples were analyzed by Tecnai G2 F20 field emission transmission electron microscope (FETEM) (Philip, Netherlands).

2 Results and Discussions

Fig.1 shows the TG/DSC curves of AIOOH sample (Sp) under optimum conditions from the ambient temperature to 1500 °C in nitrogen atmosphere. The first endothermic peak of Sp sample is formed at 392 °C. Both TG and DSC curves indicate that 23% mass loss between 220~450 °C is resulting from the loss of hydrate of $\text{AIOOH} \cdot n\text{H}_2\text{O}$. The second exothermic peak appearing at 882 °C is caused by phase transition of $\gamma\text{-Al}_2\text{O}_3 \rightarrow \theta\text{-Al}_2\text{O}_3$. Therefore, phase transition temperature of $\gamma\text{-Al}_2\text{O}_3 \rightarrow \theta\text{-Al}_2\text{O}_3$ is estimated to be about 882 °C. The third exothermic peak appearing at 1224 °C is caused by phase transition of $\theta\text{-Al}_2\text{O}_3 \rightarrow \alpha\text{-Al}_2\text{O}_3$, which corresponds to the phase transition temperature of $\theta\text{-Al}_2\text{O}_3 \rightarrow \alpha\text{-Al}_2\text{O}_3$. The last exothermic peak appears at 1396 °C, which is caused by the reduction of surface energy, and thought to be the crystal growth of $\alpha\text{-Al}_2\text{O}_3$.

Fig.2 shows TG/DSC curves of Eu^{3+} doped AIOOH sample (Sp-E). From the curves it can be seen that an endothermic peak at 122 °C results from the desorption of physical adsorbed water. The endothermic peak at 390 °C is the loss of crystal water in Sp-E sample. Above 535 °C, $\text{AIOOH} \rightarrow \gamma\text{-Al}_2\text{O}_3$ phase transition happens and Eu^{3+} ions replace Al^{3+} ions and enter the crystal lattice of $\gamma\text{-Al}_2\text{O}_3$ in the process of $\text{AIOOH} \rightarrow \gamma\text{-Al}_2\text{O}_3$ phase transition. The endothermic reaction exists when Eu^{3+} ions substitute Al^{3+} ions in the lattice of $\gamma\text{-Al}_2\text{O}_3$. Endothermic effect starts at

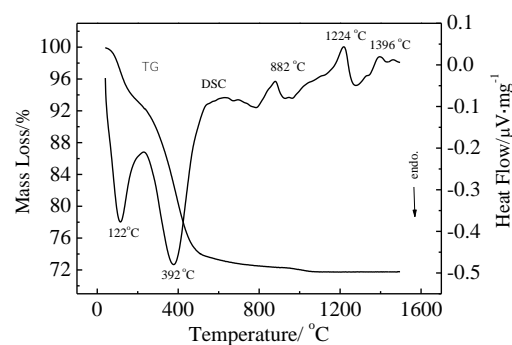


Fig.1 TG/DSC curves of AIOOH samples (Sp)

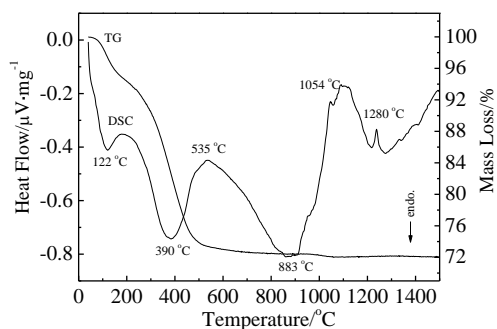


Fig.2 TG/DSC curves of Eu^{3+} doped AIOOH samples (Sp-E)

535 °C and is finished at 883 °C. There is no significant phase transition endothermic peak of $\text{AIOOH} \rightarrow \gamma\text{-Al}_2\text{O}_3$ in the temperature range of 500~900 °C. Therefore, $\text{AIOOH} \rightarrow \gamma\text{-Al}_2\text{O}_3$ phase transition temperature of Sp-E sample can't be inferred according to DSC curve. Exothermic peaks appearing at 1054 and 1237 °C are corresponding to the $\gamma\text{-Al}_2\text{O}_3 \rightarrow \theta\text{-Al}_2\text{O}_3$ and $\theta\text{-Al}_2\text{O}_3 \rightarrow \alpha\text{-Al}_2\text{O}_3$ phase transitions, respectively. Due to addition of europium ions, phase transition temperatures of $\gamma\text{-Al}_2\text{O}_3 \rightarrow \theta\text{-Al}_2\text{O}_3$ and $\theta\text{-Al}_2\text{O}_3 \rightarrow \alpha\text{-Al}_2\text{O}_3$ are apparently elevated by 172 and 13 °C, respectively.

XRD patterns of AIOOH samples Sp are shown in Fig.3. It can be summarized that the main phases are $\gamma\text{-Al}_2\text{O}_3$ with cubic structure at the sintering temperature of 600 °C, $\gamma\text{-Al}_2\text{O}_3$ and a small amount of $\theta\text{-Al}_2\text{O}_3$ with monoclinic structure at 900 °C, $\theta\text{-Al}_2\text{O}_3$ and a few $\alpha\text{-Al}_2\text{O}_3$ rhombohedral structure at 1100 °C, and single $\theta\text{-Al}_2\text{O}_3$ phase at 1300 °C. It further indicates that 882 °C and 1224 °C are the phase transition temperatures of $\gamma\text{-Al}_2\text{O}_3 \rightarrow \theta\text{-Al}_2\text{O}_3$ and $\theta\text{-Al}_2\text{O}_3 \rightarrow \alpha\text{-Al}_2\text{O}_3$, respectively. Simultaneously, diffraction peaks of $\gamma\text{-Al}_2\text{O}_3$ and $\theta\text{-Al}_2\text{O}_3$ are broadened obviously and diffraction peaks of $\alpha\text{-Al}_2\text{O}_3$ sharpen, suggesting that $\gamma\text{-Al}_2\text{O}_3$ and $\theta\text{-Al}_2\text{O}_3$ are composed of nano grains with the lower crystallinity and $\alpha\text{-Al}_2\text{O}_3$ has a higher crystallinity.

XRD patterns of Eu^{3+} doped AIOOH samples Sp-E are shown in Fig.4. From the figure it is obvious, after

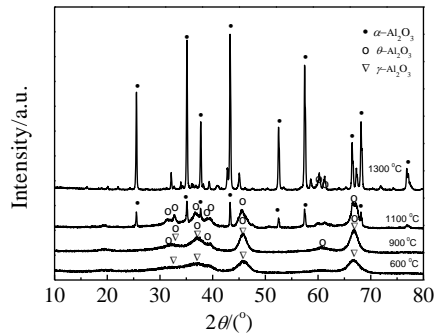


Fig.3 XRD patterns of AlOOH samples (Sp) sintered at different temperatures

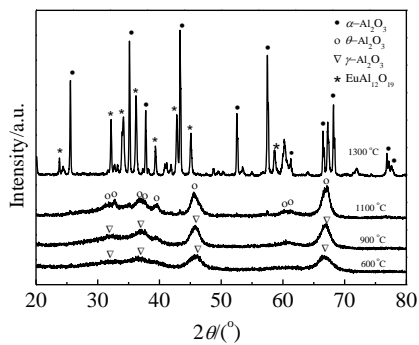


Fig.4 XRD patterns of Eu³⁺ doped AlOOH samples (Sp-E) sintered at different temperatures

calcination at 600 and 900 °C, the Sp-E samples display a cubic structure of γ -Al₂O₃. Monoclinic structure of θ -Al₂O₃ is obtained at 1100 °C, while the phase transition from γ -Al₂O₃ to θ -Al₂O₃ happens at 1054 °C as shown in Fig.2. The principal phase is α -Al₂O₃ with rhombohedral structure at 1300 °C, suggesting that the phase transition of θ -Al₂O₃→ α -Al₂O₃ occurs at 1237 °C according to Fig.2.

According to γ -Al₂O₃ and α -Al₂O₃ crystal parameters in Fig.3 and Fig.4, lattice constants (*a*, *b*, and *c*) and cell volume (*V*) of γ -Al₂O₃ and α -Al₂O₃ generated in the process of Sp and Sp-E phase transitions were calculated and are listed in Table 1. Crystal face (311) of γ -Al₂O₃ was taken to calculate the lattice constant *a* and cell volume ($V = a^3$) of γ -Al₂O₃. For orthorhombic crystals of α -Al₂O₃, (012), (110) and (113) crystal faces were chosen to calculate the lattice constants *a*, *b*, *c* and cell volumes ($V=abc$) of α -Al₂O₃.

It can be concluded from Table 1 that cell volume of γ -Al₂O₃ obtained from Sp-E sample is greater than the corresponding cell volume gained from Sp sample sintered at 600 °C and 900 °C. The main reason is that Eu³⁺ ions substitute Al³⁺ ions and enter crystal lattice of γ -Al₂O₃, resulting in an increase of γ -Al₂O₃ cell volume. According to XRD patterns in Fig.4, Eu-containing compounds are not found at 1100 °C, 900 °C and 600 °C. Eu³⁺ ions, which are in the presence of substitution doping, entirely enter γ -Al₂O₃ and θ -Al₂O₃ lattices. Cell volumes of α -Al₂O₃ generated by Sp-E and Sp sample phase transitions are similar, suggesting that the Eu³⁺ ions do not enter α -Al₂O₃ lattice, but exist wholly in the form of EuAl₁₂O₁₉.

Table 1 Lattice constants of AlOOH (Sp) and Eu³⁺ doped AlOOH (Sp-E) sintered at different temperatures

Sample	Sintering temp./ °C	Phase	<i>a</i> /nm	<i>b</i> /nm	<i>c</i> /nm	<i>V</i> /nm ³	<i>B</i> _{1/2(400)} *	<i>D</i> ₍₄₀₀₎ **
Xerogel	600	γ -Al ₂ O ₃	0.795 08	0.795 08	0.795 08	0.502 61	2.69	3.167 7
	900	γ -Al ₂ O ₃	0.799 08	0.799 08	0.799 08	0.510 24	1.76	4.841 5
	1300	α -Al ₂ O ₃	0.291 66	0.412 64	1.301 52	0.156 6	-	-
Eu doped xerogel	600	γ -Al ₂ O ₃	0.797 56	0.797 56	0.797 56	0.507 33	2.79	3.055 7
	900	γ -Al ₂ O ₃	0.803 12	0.803 12	0.803 12	0.518 01	1.90	4.487 0
	1300	α -Al ₂ O ₃	0.291 51	0.411 86	1.300 91	0.156 2	-	-

Note: *B*_{1/2(400)}*-full width at half maximum, *D*₍₄₀₀₎** -grain size

FETEM images of Eu³⁺ doped and undoped AlOOH samples Sp and Sp-E sintered at 1300 °C are shown in Fig.5. Comparing Fig.5a and Fig.5b, it is clear to see that crystallinity degree of α -Al₂O₃ is increased by Eu³⁺ doping. Additionally, it is found that the EuAl₁₂O₁₉ is formed along α -Al₂O₃ grain boundaries, which prevent the bulk diffusion of Al³⁺ ions, as shown in Fig.5b. Hence the phase transition temperature of θ -Al₂O₃→ α -Al₂O₃ is raised accordingly. This observation was also evidenced by the Ref. [26] that the EuAlO₃ compound existed between α -Al₂O₃ grain boundaries, resulting in an increase in the crystallization temperature of α -Al₂O₃ when Eu³⁺ ion was doped.

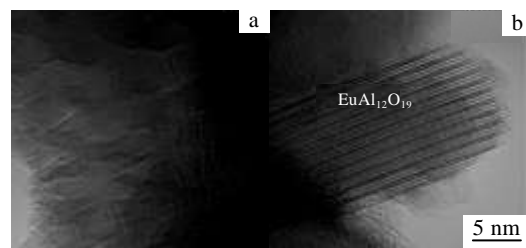


Fig.5 FETEM images of AlOOH samples (Sp) (a) and Eu³⁺ doped AlOOH samples (Sp-E) (b) sintered at 1300 °C

3 Conclusions

1) Phase transition temperatures of $\gamma\text{-Al}_2\text{O}_3 \rightarrow \theta\text{-Al}_2\text{O}_3$ and $\theta\text{-Al}_2\text{O}_3 \rightarrow \alpha\text{-Al}_2\text{O}_3$ in the phase transition process of Eu^{3+} doped AIOOH sample are raised by 172 and 13 °C, respectively. Eu^{3+} ions in the form of substitution doping replaces Al^{3+} ions and enter lattices of $\gamma\text{-Al}_2\text{O}_3$ and $\theta\text{-Al}_2\text{O}_3$. Crystallinity degree of $\gamma\text{-Al}_2\text{O}_3$ can be improved by doping Eu^{3+} ion, which may be the main reason for the elevation of $\gamma\text{-Al}_2\text{O}_3 \rightarrow \theta\text{-Al}_2\text{O}_3$ phase transition temperature.

2) Cell volume of $\alpha\text{-Al}_2\text{O}_3$ formed in the phase transition process of Eu^{3+} doped AIOOH sample is found to be essentially constant, suggesting that Eu^{3+} ions do not enter the $\alpha\text{-Al}_2\text{O}_3$ lattice, while exist in the form of $\text{EuAl}_{12}\text{O}_{19}$ compound. $\text{EuAl}_{12}\text{O}_{19}$ compound exists along $\alpha\text{-Al}_2\text{O}_3$ grains boundaries, which hinder the bulk diffusion of Al^{3+} ions. Therefore, phase transition temperature of $\theta\text{-Al}_2\text{O}_3 \rightarrow \alpha\text{-Al}_2\text{O}_3$ is increased.

References

- Boumaza, Favaro L, Le ðion J et al. *Journal of Solid State Chemistry*[J], 209, 182: 1171
- Ja Hun Kwak, Charles H, Peden F et al. *The Journal of Physical Chemistry C*[J], 2011, 115: 12 575
- Scott Nordahl C, Gary L Messing. *Thermochimica Acta*[J], 1998, 318: 187
- Jagota S, Raj R. *Journal of Materials Science*[J], 1992, 27: 2551
- Kumagai M, Messing G L. *Journal of American Ceramic Society*[J],1984, 67(11): C230
- Shelleman R A, Messing G L, Kumagai M. *Journal of Non-Crystalline Solids*[J], 1986, 82(1): 277
- Suwa Y, Komarneni S, Roy R. *Journal of Materials Science Letters*[J], 1986, 5(1): 21
- Yarbrough W A, Roy R. *Journal of Materials Research*[J], 1987, 2(4): 494
- McArdle J L, Messing G L. *Advanced Ceramic Materials*[J], 1988, 3(4): 387
- Pach L, Roy R, Komarneni S. *Journal of Materials Research*[J], 1990, 5(2): 278
- Prouzet E, Fargeot D, Baumard J F. *Journal of Materials Science Letters*[J], 1990, 9(7): 779
- Tsai D S, Hsieh C C. *Journal of American Ceramic Society*[J], 1991,74(4): 830
- Urretavizcaya G, Porto Lopez J M. *Materials Research Bulletin*[J], 1992, 27(4): 375
- Xue L A, Meyer K, Chen I W. *Journal of the American Ceramic Society*[J], 1992, 75(4): 822
- Hrabeř Z, Spaldon O M, Pach L et al. *Materials Research Bulletin*[J], 1992, 27(4): 397
- Messing G L, Kumagai M. *American Ceramic Society Bulletin*[J],1994, 73(10): 88
- Suryanarayana K V, Panda R K, Prabhu N et al. *Ceramics International*[J], 1995, 21(3) : 173
- Nordahl C S, Messing G L. *Journal of American Ceramic Society*[J], 1996, 79(12): 3149
- Wu S J, De Jonghe L C. *Journal of American Ceramic Society*[J], 1996, 79(8): 2207
- Ersoy B, Gunay V. *Ceramics International*[J], 2004, 30: 163
- Liu Yong, Chen Xiaoyin, Yang Zhuxian. *Journal of Fudan University: Natural Science*[J], 2000, 39(4): 374 (in Chinese)
- Liu Yong, Chen Xiaoyin, Niu Guoxing et al. *Chinese Journal of Catalysis*[J], 2000, 21(2): 121 (in Chinese)
- Liu Dongyan, Fan Yanzhen, Zhang Guoli et al. *Acta Physico-Chimica Sinica*[J], 2001, 17(11): 1036 (in Chinese)
- Song Zhenya, Wu Yuchen, Yang Ye et al. *Journal of Chinese Ceramic Society*[J],2004, 32(8): 920 (in Chinese)
- Wu Yuchen, Yang Ye, Li Yong et al. *Acta Physico-Chimica Sinica*[J], 2005, 21(1): 79 (in Chinese)
- Ge Cui, Huang Shuhui, Xiao Li et al. *Journal of Jilin Normal University: Natural Science Edition*[J], 2004, 3: 11 (in Chinese)

钕离子对拟薄水铝石相变和微结构的影响机理研究

朱福良¹, 蒙延双¹, 王达健²

(1. 兰州理工大学 甘肃省有色金属新材料省部共建国家重点实验室, 甘肃 兰州 730050)

(2. 天津理工大学, 天津 300384)

摘要: 拟薄水铝石溶胶中加入 $\text{Eu}(\text{NO}_3)_3$ 后, 采用喷雾干燥拟薄水铝石干凝胶。通过 TG-DSC、XRD 和 FETEM 等方法, 对比分析了 Eu 离子对拟薄水铝石相变和微结构的影响机理。结果表明, 掺杂 Eu 离子使拟薄水铝石相变过程中 $\gamma\text{-Al}_2\text{O}_3 \rightarrow \theta\text{-Al}_2\text{O}_3$ 和 $\theta\text{-Al}_2\text{O}_3 \rightarrow \alpha\text{-Al}_2\text{O}_3$ 的相变温度分别提高了 172 °C 和 13 °C。Eu³⁺ 离子全部进入 $\gamma\text{-Al}_2\text{O}_3$ 和 $\theta\text{-Al}_2\text{O}_3$ 晶格, 并提高了 $\gamma\text{-Al}_2\text{O}_3$ 结晶度, 因此提高 $\gamma\text{-Al}_2\text{O}_3 \rightarrow \theta\text{-Al}_2\text{O}_3$ 相变温度。相变生成 $\alpha\text{-Al}_2\text{O}_3$ 时, Eu 离子全部以 $\text{EuAl}_{12}\text{O}_{19}$ 存在于 $\alpha\text{-Al}_2\text{O}_3$ 晶界间阻止了 Al^{3+} 体相扩散, 因此导致 $\theta\text{-Al}_2\text{O}_3 \rightarrow \alpha\text{-Al}_2\text{O}_3$ 相变温度升高。

关键词: 拟薄水铝石; 相变; 微结构; 钕离子掺杂

作者简介: 朱福良, 男, 1975 年生, 博士, 副教授, 兰州理工大学材料科学与工程学院, 甘肃 兰州 730050, 电话: 0931-2976378, E-mail: chzfl@126.com